SegLLM: Multi-round Reasoning Segmentation with Large Language Model

Anonymous authors
Paper under double-blind review

Abstract

We present SegLLM, a novel multi-round interactive reasoning segmentation model that enhances LLM-based segmentation by exploiting conversational memory of both visual and textual outputs. By leveraging a mask-aware multimodal LLM, SegLLM re-integrates previous segmentation results into its input stream, enabling it to reason about complex user intentions and segment objects in relation to previously identified entities, including positional, interactional, and hierarchical relationships, across multiple interactions. This capability allows SegLLM to respond to visual and text queries in a chat-like manner. Evaluated on the newly curated MRSeg benchmark, SegLLM outperforms existing methods in multi-round interactive reasoning segmentation by over 20%. In addition, SegLLM obtains a 5.5% improvement in cIoU for standard single-round referring segmentation and a 4.5% increase in Acc@0.5 for referring expression comprehension.

1 Introduction

Image segmentation plays a crucial role in numerous computer vision tasks, while traditional methods have been limited to providing segmentation results for close-set categories (Cheng et al., 2022; He et al., 2017) or simple text queries (Ding et al., 2023; Wang et al., 2024b) using CLIP (Ding et al., 2023; Radford et al., 2021) or BERT (Wang et al., 2024b; Devlin et al., 2018) text embeddings as classifiers. Recent advancements in Large Vision-Language Models (LVMs) (Pi et al., 2023a; Zhang et al., 2023a; Lai et al., 2024; Wu et al., 2024; Liu et al., 2024; Touvron et al., 2023; Alayrac et al., 2022; Awadalla et al., 2023; Dai et al., 2024) have reformulated image segmentation as a next token prediction task, enabling segmentation models to engage in natural language conversations with users and reason about the presence, location, and relationships of objects in complex visual scenes. For instance, LISA (Lai et al., 2024), a Language Instructed Segmentation Assistant, produces segmentation masks by incorporating a [SEG] token into its vocabulary, which, when generated, is decoded into the corresponding segmentation mask.

These LLM segmentation models (Lai et al., 2024; Wu et al., 2024; Pi et al., 2023a; Zhang et al., 2023a) typically achieve their localization capabilities by incorporating a decoder that converts the output [SEG] tokens of LLMs into localization results. They are trained on numerous visual queries such as "please find the heart healthy food in the image", where responses include both text outputs and segmentation masks. Essentially, these models are advanced versions of early open-vocabulary segmentation models, with their text encoders upgraded from smaller language models, such as BERT (Devlin et al., 2018), to smarter LLMs, such as Llama (Touvron et al., 2023). Consequently, LLM segmentation models are often evaluated on traditional referring expression segmentation (RES) datasets, such as RefCOCO, which provide a single text query corresponding to each mask. These single-round referring expression segmentation (RES) datasets overlook one of the most remarkable properties of LLMs (Achiam et al., 2023; Team et al., 2023; Touvron et al., 2023; Jiang et al., 2023): generating multi-round responses in a conversational manner. In this paper, we intend to answer the question: *can segmentation models reason about previously segmented objects and conversations, responding to multiple visual and text queries in a chat-like manner?*

Current LLM segmentation or detection models (Lai et al., 2024; Zhang et al., 2023a; Wu et al., 2024), despite their impressive single-round performance, fall short as multi-modal conversation agents due to their inability to handle multi-round, interactive conversations. For instance, after obtaining a mask of a *'person in black hoodie'* in Fig. 1, a user might want to perform additional

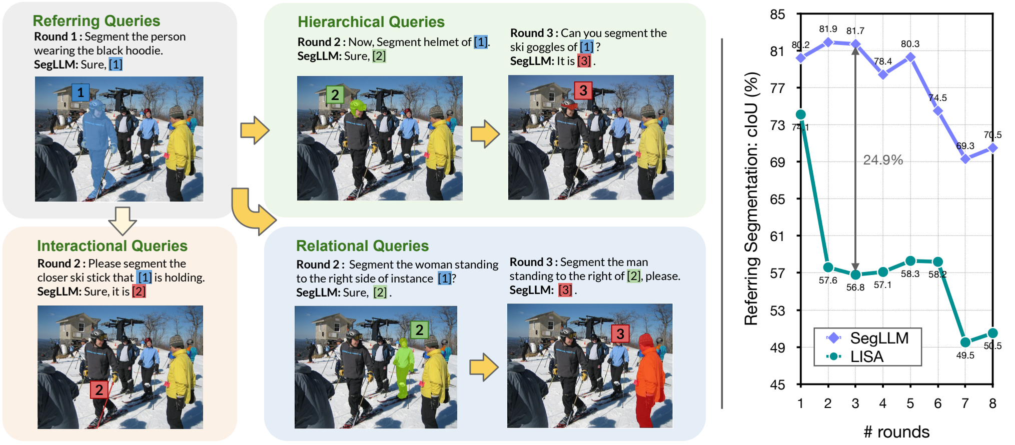

Figure 1: We present SegLLM, a multi-round interactive reasoning segmentation model designed to engage in chat-like interactions by responding to both visual and text queries. It reasons about previously segmented objects and conversations to understand complex user intentions. **On the left**: SegLLM can infer intricate relationships between objects, such as positional, interactional, and hierarchical connections with previously identified entities, *e.g.*, instance [1]. **On the right**: We introduce the MRSeg, a new multi-round image referring segmentation benchmark. As the rounds progress, the complexity of interaction and memory retention increases, leading to a decline in performance as measured by cIoU. However, SegLLM consistently surpasses the previous state-of-the-art method LISA (Lai et al., 2024), with a significant margin across all conversational rounds.

queries based on this mask output—such as segmenting the *'ski he is holding'*, segmenting the *'man standing to the right of him'*, or segmenting a different person if the output is incorrect. Existing models struggle with these complex queries because there is no "communication" between the large language models (LLMs) and the vision encoders. Information flows only from the LLMs to the mask decoder, not vice versa, preventing the LLM from being aware of the output mask and making it difficult to reason about complex queries involving previous mask outputs.

To address this issue, we propose **SegLLM**. Unlike existing LLM segmentation models that naively assemble a mask decoder with an LLM, we introduce a novel communication protocol that feeds the segmentation outputs of the mask decoder back into the input stream of the LLMs, and the past conversation context into the input query of the mask decoder. This design allows the LLMs to "see" past mask outputs and the mask decoder to "see" the past conversation context, enabling it to handle complex queries like *'segment the helmet of the previously segmented person'*, as shown in Fig. 1. Concretely, we introduce a Mask-Encoding scheme to make the LLM mask-aware and a Reference Mask-Decoding scheme to make the segmentation head context-aware. To fully explore the capabilities of these novel designs, we curated multiple high-quality multi-round interactive segmentation datasets, named **MRSeg**. The new dataset consists of complex object queries involving existing mask outputs, formulated in seamless multi-round natural language conversations.

Through extensive experiments, we demonstrate that SegLLM outperforms previous state-of-the-art models by 18∼30% on our multi-round reasoning segmentation benchmarks, MRSeg. Additionally, SegLLM surpasses prior state-of-the-art performance on the single-round referring segmentation and detection benchmark, RefCOCO, with over a 5.5% improvement in segmentation (cIoU) and a 4.5% increase in detection accuracy (Acc@0.5). SegLLM also exhibits greater robustness to various question templates, achieving 9.6% performance gains on RefCOCO with diverse query formats. These results establish SegLLM as a versatile model for a broad range of instruction-following segmentation tasks, adept at processing multiple visual and text queries in a conversational manner.

2 Related Works

2.1 Multi-modal Large Language Models

To leverage the advancements in language models (Brown et al., 2020; Touvron et al., 2023; Chowdhery et al., 2023; Le Scao et al., 2023; Hoffmann et al., 2022) across various modalities, Multi-modal

Large Language Models (MLLMs) have been developed to combine language and vision (Yin et al., 2023; Liu et al., 2024; Zhu et al., 2023; Alayrac et al., 2022). Flamingo was one of the first unified architectures to align image and text pairs in context learning through gated cross-attention blocks (Alayrac et al., 2022). End-to-end MLLMs typically require a finetuning process where an intermediate network (Lai et al., 2024; Zhang et al., 2023a) and/or sampler module (You et al., 2023) is used to map the vision features into the language space. BLIP-2 bridges the modality gap with a querying transformer and a two-stage training process, which involves pretraining on a trainable LLM and instruction tuning on a frozen one (Li et al., 2023b). Models like MiniGPT-4 (Zhu et al., 2023) and LLava (Liu et al., 2024) follow a similar training paradigm, with Vicuna 18 as a language decoder and GPT-4 designed prompts. Other notable models in instruction tuning include Otter (Li et al., 2023a) that is based on (Awadalla et al., 2023), mPLUG-Owl (Ye et al., 2023) with a novel modular architecture, and InstructBLIP (Dai et al., 2024) which features an instruction aware Q-former.

2.2 Multi-round Conversational MLLMs

Recent advancements in MLLMs have focused on enhancing interactive capabilities. Models like Kosmos-2 (Peng et al., 2023) and Shikra (Chen et al., 2023) use visual grounding and referring to provide the LLM with detailed location information of the objects, which enables the user to point out specific areas in the image. Various works aim to improve local information, such as Ferret (You et al., 2023) and PerceptionGPT (Pi et al., 2023b) which employ flexible continuous representations to handle different shapes. Other approaches (Yang et al., 2023a;b; Zeng et al., 2022) utilize prompt engineering and APIs to facilitate interaction, instead of relying on end-to-end models. More recent approaches introduce the concept of reasoning, leveraging LLMs to provide a visual answer based on implied information. DetGPT (Pi et al., 2023a) performs object detection using high-level instructions rather than distinct classes. GPT4RoI (Zhang et al., 2023b) receives spatial boxes as input to focus on specific regions and better align vision and text. LISA (Lai et al., 2024) adds a new embedding prompt to the mask decoder of the SAM (Kirillov et al., 2023) guiding segmentation, which is then processed by LLaVA (Liu et al., 2024) to perform high-level reasoning. NExT-Chat (Zhang et al., 2023a) expands on LISA by using embeddings instead of tokens for location information and adding a decoder with a joint loss to facilitate object detection.

While some methods support multi-round conversations, they often lack mechanisms to maintain localization performance over successive rounds, leading to degradation and information loss. SegLLM improves the multi-round interactive segmentation by leveraging the text and segmentation results from previous rounds, thereby generating refined masks and supporting hierarchical representations to enhance performance in multi-round interactions.

3 Background: Reasoning Segmentation

Task definition. The reasoning segmentation task (Lai et al., 2024) involves generating binary segmentation masks based on an image and descriptive, free-form text prompts. This task requires the model to possess cross-modality comprehension, understanding both the complex visual scenes, as well as the natural-language signals in the text prompt. Specifically, the model must interpret complex user text prompts that go beyond simple class names to include implicit descriptions that require general world knowledge, such as “the device that can illuminate a dark room”.

Overall pipeline. To achieve such capabilities, reasoning segmentation model typically first employs a pre-trained large multimodal models (VLMs), $\mathcal{F}_{\text{MM}}$, which is capable of comprehending both visual and textual information simultaneously (Lai et al., 2024). A new [SEG] token is then added to the VLMs's vocabulary. Given an input image x_{img} and input text prompt x_{txt}, the VLMs generates an output text response $\hat{y}_{\text{txt}}$, which includes the [SEG] token to request the generation for a segmentation mask. Finally, the segmentor $\mathcal{F}_{\text{SEG}}$ uses the last layer's hidden state, h_{seg}, corresponding to the [SEG] token along with the input image x_{img} to generate the segmentation mask $\hat{y}_{\text{SEG}}$.

Model architecture. An image reasoning segmentation model, $\mathcal{F}_{\text{MM}}$, typically consists of three key components (Lai et al., 2024): an image encoder $\mathcal{E}_{\text{MM}}$ (*e.g.*, CLIP (Radford et al., 2021) and DINOv2 (Oquab et al., 2023)), a base language model $\mathcal{L}$ (*e.g.*, Llama (Touvron et al., 2023)), and a vision-to-language projection layer f_{VtoL}, which is typically an MLP layer. Given a pair of input image and text prompt $(x_{\text{img}}, x_{\text{txt}})$, the image encoder first encodes the input image into patch embeddings

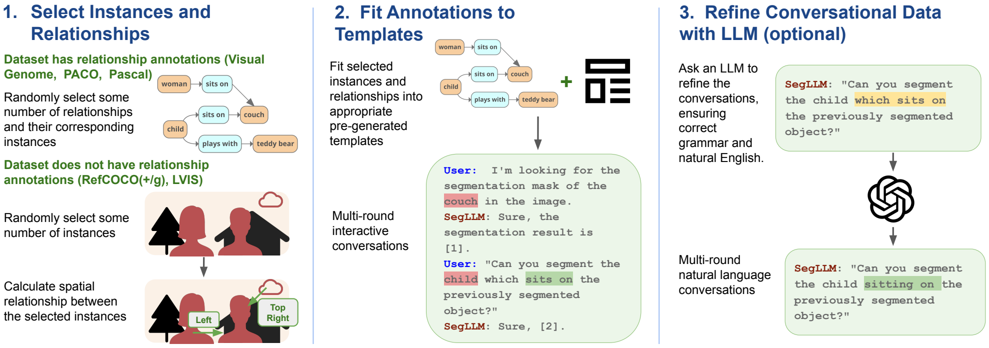
1. Select Instances and Relationships
Dataset has relationship annotations (Visual Genome, PACO, Pascal)
Randomly select some number of relationships and their corresponding instances
woman
sits on
couch
child
sits on
plays with
teddy bear
Dataset does not have relationship annotations (RefCOCO(+/g), LVIS)
Randomly select some number of instances
Calculate spatial relationship between the selected instances
Left
Top Right
2. Fit Annotations to Templates
Fit selected instances and relationships into appropriate pre-generated templates
Multi-round interactive conversations
3. Refine Conversational Data with LLM (optional)
Ask an LLM to refine the conversations, ensuring correct grammar and natural English.
Multi-round natural language conversations

User: I'm looking for the segmentation mask of the couch in the image.
SegLLM: Sure, the segmentation result is [1].
User: "Can you segment the child which sits on the previously segmented object?"
SegLLM: Sure, [2].

SegLLM: "Can you segment the child which sits on the previously segmented object?"

SegLLM: "Can you segment the child sitting on the previously segmented object?"

Figure 2: Pipeline for generating our multi-round conversational dataset MRSeg. The workflow involves selecting instances, generating relationships, fitting the instances and relationships into conversational templates, and refining the conversations using a language model for improved accuracy.

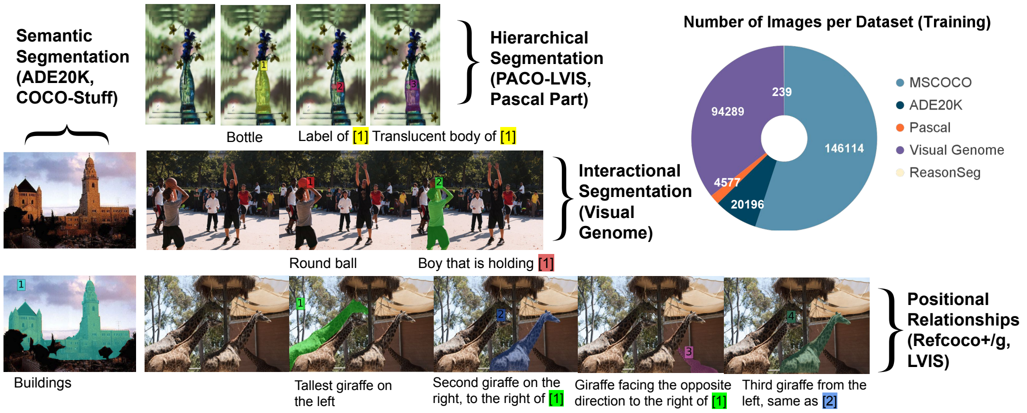

Figure 3: Statistics and sample conversations for the Multi-Round Referring Segmentation dataset (MRSeg). We provide more details for MRSeg in Appendix A.5.

h_{img}, which are then projected into the text embedding space via f_{VtoL}. The resulting visual tokens are concatenated with the sequence of text tokens h_{txt}. Finally, taking both visual and language tokens as inputs, the language model $\mathcal{L}$ produces the output response $\hat{y}_{\text{txt}}$ containing the [SEG] token: $\hat{y}_{\text{txt}} = \mathcal{F}_{\text{MM}}(x_{\text{img}}, x_{\text{txt}}) = \mathcal{L}(\text{cat}([f_{\text{V2L}}(\mathcal{E}_{\text{MM}}(x_{\text{img}})), h_{\text{txt}})])$. The [SEG] token in the output responses is then decoded into the segmentation mask using the mask decoder $\mathcal{F}_{\text{SEG}}$ of a pre-trained segmentation model, SAM (Kirillov et al., 2023): $\hat{y}_{\text{SEG}} = \mathcal{F}_{\text{SEG}}(x_{\text{img}}, h_{\text{SEG}}) = \mathcal{D}_{\text{SEG}}(\mathcal{E}_{\text{SEG}}(x_{\text{img}}), h_{\text{SEG}})$.

4 Multi-round Reasoning Segmentation

The success of our **SegLLM** method relies on two essential components: a comprehensive dataset **MRSeg** that has an extensive collection of **M**ulti-**R**ound interactive **Seg**mentation instructions, and a mask-aware VLMs specifically designed to reason about the conversational history, with a particular focus on the segmentation masks generated in previous interactions.

4.1 Data Pipeline

Data sources. We constructed our multi-round image reasoning segmentation dataset (MRSeg) based on several widely utilized datasets, and include data from the following sources: RefCOCO(+/g) (Yu et al., 2016; Kazemzadeh et al., 2014), Visual Genome (Krishna et al., 2017), PACO-LVIS (Ramanathan et al., 2023), LVIS (Gupta et al., 2019), Pascal Panoptic Part (de Geus et al., 2021), ADE20K(Zhou et al., 2017), COCO-Stuff(Caesar et al., 2016) and MSCOCO(Lin et al., 2014b). We used bounding box or segmentation annotations from these datasets to generate natural language conversations, applying a template-based approach as detailed in subsequent sections. The overall pipeline can be seen in Fig. 2 and we provide the statistics and some sample data for MRSeg in Fig. 3.

Multi-round conversation generation. We design various pipelines for generating multi-round conversations, tailored to the types of data and inter-instance relationships they support:

- **Hierarchical Relationships** (PACO-LVIS, Pascal Panoptic Part): In these queries, the model is tasked with segmenting objects that are sub-parts of previously segmented instances. The queries start by asking about the instance, followed by questions about its parts. Example query: *"Can you segment the <part> of the <object>?"*
- **Positional Relationships** (RefCOCO(+/g), LVIS): These queries require the model to segment objects based on their positional relationships to previous outputs. An example query is: *"Can you segment the <class> that is <relationship> the output from round <i>?"* We refine these conversations using GPT-4 (our full prompt to GPT-4 can be found in Table A3) to ensure natural language fluency. Details on the RefCOCO(+/g) pipeline are in Fig. A2. Additionally, we introduce a challenging variant called MRSeg (hard), where understanding previous round information is necessary to correctly segment the current instance (details in Appendix A.5).
- **Interactional Relationships** (Visual Genome): Utilizing Visual Genome (VG) relationship annotations, we construct conversations that focus on interactional dynamics, rather than just positional relationships. Each conversation has two rounds: the first round segments the subject, and the second round segments an object based on its relationship to the subject.
- **Attribute-oriented Queries** (MSCOCO): These queries ask the model to segment objects based on their attributes or usage rather than class names. An example query is: *Q: Outline and extract the object that has a tall, slender neck covered with a distinct pattern of patches. A: Yes, the figure you specified for segmentation is a giraffe*. We generate captions by cropping MSCOCO instances and using GPT-4V prompts (details in Table A2).
- **Single-Round Semantic Segmentation** is based on ADE20K and COCO-Stuff datasets. We construct single-round conversations by fitting class labels into various query templates.

Additional details on the multi-round data pre-processing for MRSeg are provided in Appendix A.5. For better generalization, we generated a custom set of diverse questions templates using GPT-4. Please refer to Appendix A.2 for more details.

4.2 SegLLM for Multi-round Image Reasoning Segmentation

Overall Pipeline. We introduce SegLLM to ensure that the VLMs's next token predictions can incorporate the conversational memory from previous interactions, including the visual outputs, *i.e.*, segmented masks, and the text conversations. The architecture of our model is illustrated in Fig. 4. SegLLM consists of two key components: 1) Mask-Encoding Module: This module feeds the output masks back into the input stream of the LLM, enabling it to reason about segmented masks from previous rounds. 2) Mask-Aware Decoding Module: This module allows the mask decoder to generate new masks based on both the visual and textual conversational history, enhancing its contextual understanding. For example, when a user requests segmentation of a part of an object identified in a previous round (*e.g.*, the ear of a man), the model's ability to access prior mask data enables the decoder to more precisely localize and segment the specified object.

Mask-Encoding Module. For each mask generated by the decoder, we compute two types of embeddings: mask embedding and bounding box embedding. The mask embedding captures the semantic information of the masked object, and the bounding box embedding captures its location within the original image. Employing mask embeddings (one token per mask) and box tokens instead of a new set of patch tokens for each mask substantially reduces the number of visual tokens required for multi-round conversations. Furthermore, since the visual patch tokens for the entire image have already been utilized in previous conversations, this design does not compromise the richness of information necessary for accurate image segmentation and visual question answering. For more details on obtaining these embeddings during training and inference, please refer to Appendix A.3.

Mask-Aware Decoding Module. To facilitate the decoding process, we generate two tokens [REF] and [SEG] to the mask decoder, containing information about the reference mask and the target mask, respectively. For example, in the query "segment the head of *[instance 1]*" where "*[instance 1]*" is a previously segmented person, the [REF] token should encode the previous mask *[instance 1]* while [SEG] should encode the target mask. In the training process, we construct two queries. We match first query "[REF] , [PAD] " to the referenced mask M_{ref} (*[instance 1]* in the previous example), and match the second query "[REF] , [SEG] " to the desired mask M_{tgt} (the head of the person in the

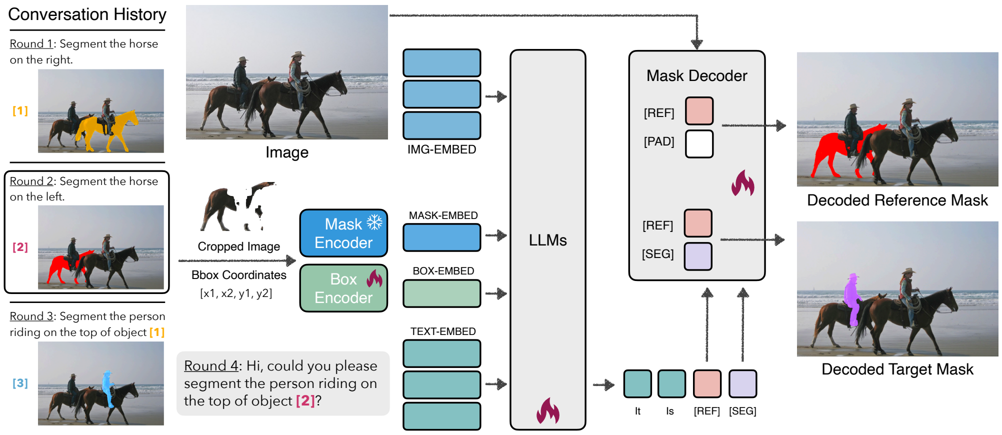

Figure 4: Model architecture of SegLLM for multi-round interactive image reasoning segmentation, which can understand complex user intentions and segment entities based on their relationships with previously identified ones. To facilitate this, first, we implement a mask encoding scheme that reincorporates the reference mask information back into the input stream of the LLMs. This enables the LLMs to reason about segmented masks from previous rounds. Second, we develop a mask-aware decoding scheme that allows the mask decoder to generate new masks based on both the output from the LLMs and the historical memory of output masks. The model uses the last layer hidden states associated with the [REF] and [SEG] tokens to generate both the reference mask and the target mask, seamlessly integrating past and current segmentation results.

previous example). The final loss is formulated as:

$$L_{\text{mask}} = L_{\text{seg}}(F([\text{REF}]\ , [\text{PAD}]\ , M_{\text{ref}})) + L_{\text{seg}}(F([\text{REF}]\ , [\text{SEG}]\ , M_{\text{tgt}})) \tag{1}$$

where $L_{\text{seg}} = L_{\text{ce}} + \lambda L_{\text{DICE}}$. We apply cross entropy loss and DICE loss to the target mask and reference mask predictions. We set λ as 1 by default.

5 Experiments

5.1 Implementation Details

We use a pretrained CLIP-ViT-Large (Radford et al., 2021) with a patch size of 14 as the image encoder, HIPIE-R50 (Wang et al., 2024b) as the mask encoder and LLaVA-v1.5-7B (Liu et al., 2024) as the base language model. Compared with LISA, which has exactly one mask per training sample, SegLLM's setup contains multiple masks per conversation. Hence, we replaced the SAM ViT-H mask decoder (Kirillov et al., 2023) with a smaller HIPIE-R50 (Wang et al., 2024b) to reduce the computation overhead during the training, We then fine-tune the LLM model and the projector weights f_{V2L} using the training set of our own multi-round instruction-segmentation dataset MRSeg, while keeping the weights of the CLIP image encoder and the HIPIE mask decoder frozen. For further implementation details, please refer to Appendix A.1.

5.2 Evaluation

Evaluation benchmarks. For standard single-round image reasoning segmentation and detection tasks, we evaluate our model on the widely used referring segmentation and comprehension benchmarks, RefCOCO/+/g (Yu et al., 2016). We also conduct qualitative and quantitative comparisons with previous SOTA models on our multi-round referring segmentation benchmarks, based on MSCOCO (Lin et al., 2014a), PACO (Ramanathan et al., 2023) and LVIS (Gupta et al., 2019), which assess performance based on positional, interactional or hierarchical relationship queries.

Evaluation metrics. We use mean Intersection-Over-Union (mIoU) and cumulative Intersection-Over-Union (cIoU) as our main evaluation metrics. To assess the model's performance across multiple rounds of conversation, we track the mIoU and cIoU scores for each round's segmentation outputs.

Rounds	MR-RefCOCO				MR-RefCOCO+				MR-RefCOCOg			
	LISA	GLaMM	SegLLM	Δ	LISA	GLaMM	SegLLM	Δ	LISA	GLaMM	SegLLM	Δ
# 2	60.6	59.5	**81.9**	**+21.3**	51.4	52.9	**78.0**	**+25.1**	61.3	65.4	**79.2**	**+13.8**
# 3	58.9	61.6	**81.7**	**+20.0**	51.2	58.3	**78.5**	**+20.2**	52.1	57.8	**76.0**	**+18.2**
# 4	61.3	59.3	**78.4**	**+17.1**	49.0	54.2	**74.3**	**+20.1**	56.0	55.4	**77.1**	**+15.0**
# 5	61.0	62.6	**80.3**	**+17.6**	48.5	50.5	**76.5**	**+26.0**	47.5	49.4	**66.9**	**+14.0**
# 6	60.7	62.6	**74.5**	**+11.9**	45.6	54.8	**73.4**	**+18.6**	39.9	40.8	**68.9**	**+24.8**
# 7	54.4	52.1	**69.3**	**+14.9**	42.8	48.4	**64.0**	**+15.6**	55.1	57.8	**71.0**	**+13.3**
# 8	51.9	50.7	**70.5**	**+18.7**	36.9	43.6	**59.0**	**+15.4**	36.3	38.4	**54.9**	**+16.5**

Table 1: Multi-round referring segmentation on the proposed multi-round RefCOCO/+/g benchmarks. As the rounds progress, it becomes harder to interact and retain all relevant information, causing the performance measured in cIoU to drop. SegLLM can consistently outperform LISA (Lai et al., 2024) and GLaMM (Rasheed et al., 2024), across a series of rounds by a significant margin on the MR-RefCOCO/+/g benchmarks.

Methods	RefCOCO			RefCOCO+			RefCOCOg	
	val	testA	testB	val	testA	testB	val	test
VLT (Ding et al., 2021)	67.5	70.5	65.2	56.3	61.0	50.1	55.0	57.7
LAVT (Yang et al., 2022)	72.7	75.8	68.8	62.1	68.4	55.1	61.2	62.1
SEEM (Zou et al., 2023)	-	-	-	-	65.7	-	-	-
LISA-7B (Lai et al., 2024)	74.1	76.5	71.1	62.4	67.4	56.5	66.4	68.5
NExT-Chat (Zhang et al., 2024)	74.7	78.9	69.5	65.1	71.9	56.7	67.0	67.0
SegLLM (ours)	**80.2**	**81.5**	**75.4**	**70.3**	**73.0**	**62.5**	**72.6**	**73.6**

Table 2: Comparison between SegLLM and baseline methods on referring segmentation. Although not specifically designed for single-round referring segmentation, the diverse and challenging multi-round referring segmentation tasks and training data enable SegLLM significantly outperforms previous state-of-the-art methods on standard referring segmentation tasks by a substantial margin. We use cIoU as the main evaluation metric.

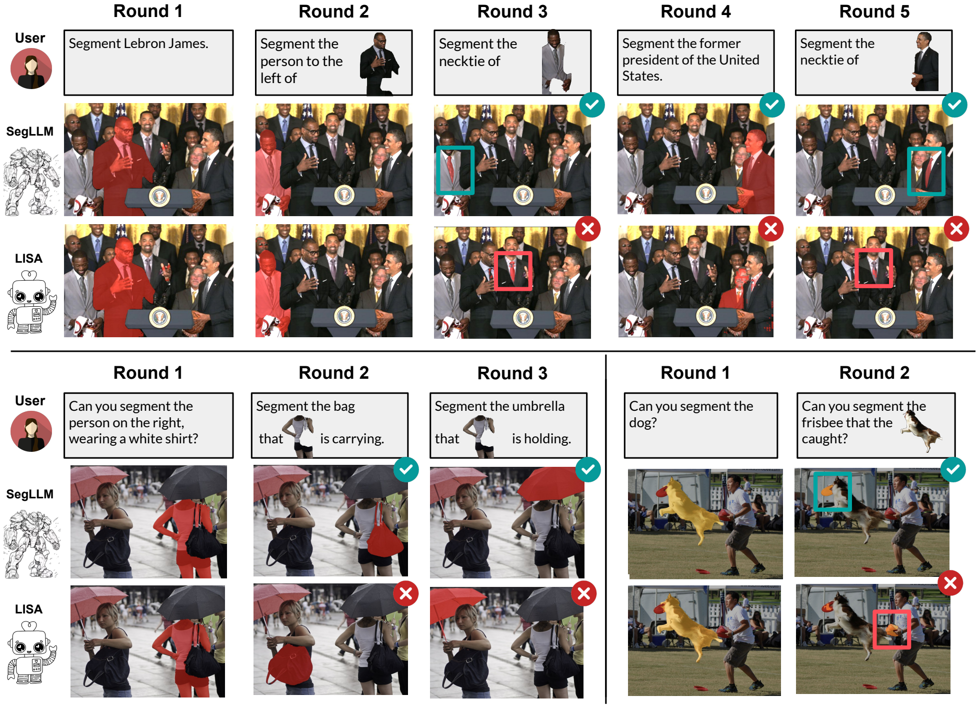
Round 1
Round 2
Round 3
Round 4
Round 5
User
Segment Lebron James.
Segment the person to the left of
Segment the necktie of
Segment the former president of the United States.
Segment the necktie of
SegLLM
LISA
Round 1
Round 2
Round 3
Round 1
Round 2
User
Can you segment the person on the right, wearing a white shirt?
Segment the bag that is carrying.
Segment the umbrella that is holding.
Can you segment the dog?
Can you segment the frisbee that the caught?
SegLLM
LISA

Figure 5: Side-by-side qualitative comparison with LISA's (Lai et al., 2024) on multi-round interactive segmentation. SegLLM not only excels in reasoning segmentation, demonstrating an understanding of world knowledge including recognition of famous individuals, as illustrated in the round 1 and round 4 results of the first demo in row one, but it also efficiently responds to questions that reference previous rounds.

5.3 Evaluation Protocol for Baseline Methods

Since some baseline models, *e.g.*, LISA, do not natively support multi-round interactive segmentation, for comparisons, we adapt our multi-round validation data into their supported single-turn format by converting the N-turn data into N single-turn instruction segmentation tasks.

Evaluation protocol for LISA. Given an example query in the MR-RefCOCO dataset "Segment the person to the left of `<mask>` `<box>`.", where `<mask>` `<box>` are encoding tokens corresponding

	LISA 1	**LISA 2**	**LISA 3**	**SegLLM**
round 2	60.6	55.9	58.9	81.9
round 3	58.9	54.7	56.8	81.7
round 4	61.3	56.7	58.8	78.4
round 5	61.0	57.8	59.7	80.3
round 6	60.7	57.7	57.4	74.5
round 7	54.4	45.6	51.0	69.3
round 8	51.9	50.3	50.1	70.5

Table 3: Evaluating LISA on MR-RefCOCO val-split by replacing the reference mask and bounding box tokens with: 1) the word "mask", 2) the captions for the reference instance, and 3) painting the reference mask onto the input image. SegLLM out performs LISA on all three approaches. For more discussion on these results, please refer to Appendix A.4

Methods	RefCOCO			RefCOCO+			RefCOCOg	
	val	testA	testB	val	testA	testB	val	test
Shikra-13B (Chen et al., 2023)	87.8	91.1	81.8	82.9	87.8	74.4	82.6	83.2
VisionLLM-H (Wang et al., 2024a)	-	86.7	-	-	-	-	-	-
Shikra-7B (Chen et al., 2023)	87.0	90.6	80.2	81.6	87.4	72.1	82.3	82.2
NExT-Chat-7B (Zhang et al., 2024)	85.5	90.0	77.9	77.2	84.5	68.0	80.1	79.8
SegLLM-7B (ours)	**90.0**	**92.1**	**86.2**	**82.2**	**85.5**	**76.1**	**83.9**	**85.9**

Table 4: Comparison between SegLLM and baseline models on referring expression comprehension (REC). SegLLM not only sets a new SOTA result in referring segmentation (Table 2), but also surpasses baseline models in detection tasks, including those specifically optimized for these tasks, such as NExT-Chat-7B (Zhang et al., 2024), or models with larger LLMs like Shikra-13B (Chen et al., 2023). The evaluation metric used is the standard detection metric for REC, Acc@0.5.

Method	**Val**		**Test**		**Test** (long query)	
	mIoU	cIoU	mIoU	cIoU	mIoU	cIoU
LISA (Lai et al., 2024)	53.6	52.3	48.7	48.8	49.2	48.9
SegLLM	**57.2**	**54.3**	**52.4**	48.4	**55.9**	**54.2**

Table 5: Result comparison on the **ReasonSeg dataset**. SegLLM demonstrates superior performance, particularly on the long query subset.

to the reference instance "the dog chasing after a butterfly", we employed the following conversions: 1) substitute `<mask> <box>` with the word "mask" to obtain "Segment the person left to the mask."; 2) substitute `<mask> <box>` with the description of the reference instance to obtain "Segment the person left to the dog chasing after a butterfly."; 3) paint the reference mask onto the input image and use "Segment the person left to the object highlighted in yellow." as the text input.

As shown in Table 3, SegLLM outperforms LISA across all three approaches on MR-RefCOCO. In our main table, Table 1, we report LISA's performance on our MR-RefCOCO/+/g benchmark using the best approach for LISA, approach 1.

Evaluation protocol for GLaMM. GLaMM natively supports an additional bounding box coordinate input, in addition to image and text. Therefore, we provided the bounding box coordinates of the reference instance, the image and the text instruction to GLaMM.

5.4 Evaluation Results

Mutli-round referring segmentation. We compare the performance of SegLLM and LISA on our multi-round referring segmentation benchmarks, MR-RefCOCO/+/g. As shown in Table 1, compared to LISA (Lai et al., 2024) and GLaMM (Rasheed et al., 2024), SegLLM not only achieves 14$\sim$26% higher cIoU score across all conversation rounds but also stays stable, whereas LISA and GLaMM's performance tends to degrade in the later turns of the conversation. For example, by round 5, the performance gap between SegLLM and GLaMM widens significantly, reaching over 17.6%, 26.0%, and 14.0% on MR-RefCOCO, MR-RefCOCO+, and MR-RefCOCOg, respectively—nearly double the gap observed in round 1 (Table 2). Besides the quantitative results, Fig. 5 presents the qualitative results comparing SegLLM with LISA (Lai et al., 2024).

Why does SegLLM's **performance in later rounds sometimes exceed the first round** by 2$\sim$4% (Table 2)? This improvement is attributed to earlier rounds helping to narrow down the search space in the image, thus enhancing the model's accuracy in subsequent queries.

Single-round referring segmentation and expression comprehension. As shown in Tabs. 2, 4 and 5, SegLLM consistently exceeds previous SOTA methods, such as LISA (Lai et al., 2024), NExT-Chat (Zhang et al., 2024) and Shikra-13B (Chen et al., 2023), in the standard single-round referring segmentation and expression comprehension tasks, despite not being specifically designed for these tasks. We hypothesize that SegLLM's ability to understand the relative relationships among objects or parts within images in multi-round tasks significantly enhances its overall visual comprehension.

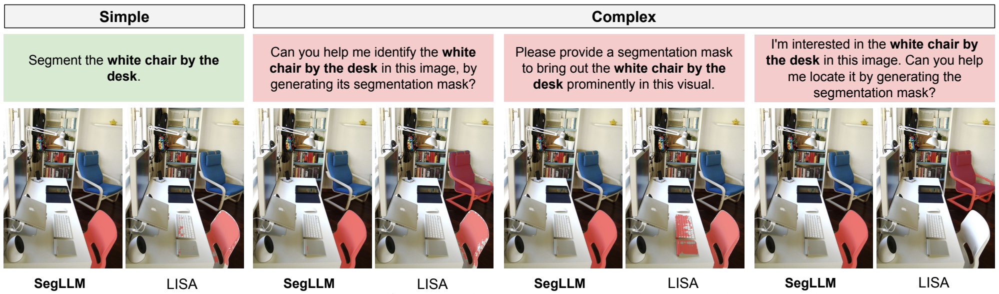
Simple
Complex
Segment the **white chair by the desk**.
Can you help me identify the **white chair by the desk** in this image, by generating its segmentation mask?
Please provide a segmentation mask to bring out the **white chair by the desk** prominently in this visual.
I'm interested in the **white chair by the desk** in this image. Can you help me locate it by generating the segmentation mask?
SegLLM
LISA
SegLLM
LISA
SegLLM
LISA
SegLLM
LISA

Figure 6: Demo results that demonstrate SegLLM's robustness against varying question queries, in contrast to LISA (Lai et al., 2024), which is sensitive to prompt phrasing. Even with simple questions presented in different templates, LISA's performance significantly declines, frequently failing to deliver correct segmentation results for most test templates. This limitation forces users to adhere to specific phrasing, such as "Segment [object descriptions]", substantially restricting the model's real-world applicability.

Models	Multi-Round PACO (w/ LVIS) (mIoU)			Multi-Round PACO (w/ LVIS) (cIoU)		
	LISA	SegLLM	Absolute Δ	LISA	SegLLM	Absolute Δ
round 1	34.7	**54.9**	**+20.2**	45.6	**65.3**	**+19.7**
round 2	10.6	**37.6**	**+27.0**	15.5	**49.7**	**+34.2**
round 3	13.7	**32.9**	**+19.1**	21.3	**40.9**	**+19.6**
round 4	11.5	**33.3**	**+21.7**	18.7	**39.4**	**+20.7**
round 5	11.6	**31.6**	**+20.0**	20.5	**41.9**	**+21.4**

Table 6: Single-round referring segmentation and multi-round hierarchical image segmentation. The Multi-Round PACO (MR-PACO) benchmark presents a significant challenge as it demands a good hierarchical understanding and the capability to precisely segment tiny masks representing parts or subparts of an object (refer to hierarchical query demos in Fig. 1). SegLLM significantly improve performance over LISA (Lai et al., 2024), demonstrating substantial improvements in both mIoU and cIoU metrics across conversation rounds.

This enhanced visual understanding capability transfers to superior performance in single-round tasks as well. However, it is worth noting that while SegLLM shows improved performance in single-round tasks, the performance gap is smaller compared to the improvements observed in multi-round tasks.

Multi-round hierarchical segmentation result comparison between SegLLM and LISA is conducted with our MR-PACO. As detailed in Sec. 4.1, each subsequent round may query a part or subpart of a whole object from a previous round of conversation. As shown in Table 6, compared to LISA, SegLLM obtains 10.7%∼16.2% higher mIoU and 13.2∼27.1% higher cIoU across all rounds. It is observed that the absolute model performance typically decreases in later rounds. This decline is primarily due to the progressively smaller object sizes (segment parts of an instance) in later rounds of the multi-round hierarchical segmentation task. As shown in Fig. 5, SegLLM leverages multi-round segmentation, using previous outputs to accurately identify the necktie of the person in the gray suit in round 2, as requested by the user. In contrast, LISA, lacking this contextual awareness, fails to correctly identify the person. This is further demonstrated in round 5, where SegLLM successfully segments Barack Obama's necktie from round 4, while LISA fails again.

Robustness against question templates. We observed that many previous studies in image reasoning segmentation, such as LISA (Lai et al., 2024) and SESAME (Wu et al., 2024), tend to overfit to the specific question templates used during training. Consequently, when these models are evaluated with diverse question templates not encountered during training, performance often significantly declines. For example, as shown in Table 7, the performance of LISA and SESAME drops by approximately 7% and 13%, respectively, when assessed using our varied templates.

To mitigate this, we intentionally diversified our question templates during the dataset generation process. As a result, our SegLLM model not only demonstrates consistent segmentation performance across diverse templates but also achieves a 5.5% higher cumulative Intersection-Over-Union (cIoU). Fig. 6 shows that LISA's performance significantly drops when asked with simple questions presented in various templates, frequently failing to produce correct segmentation results for most test templates.

5.5 Ablation Study

Ablation study. We conduct an ablation study (Table 8) on our Multi-Round RefCOCO benchmark to evaluate the effectiveness of the three components we introduced in Sec. 4.2. We assess model

Methods	**Averaged**			Diverse			LISA			SESAME		
	RC	RC+	RCg	RC	RC+	RCg	RC	RC+	RCg	RC	RC+	RCg
SESAME (Wu et al., 2024)	67.4	57.9	61.4	66.0	56.9	60.6	61.4	51.6	55.6	74.9	65.1	67.9
LISA-7B (ft) (Lai et al., 2024)	70.1	61.0	63.0	67.8	59.0	62.4	**74.7**	**64.9**	66.1	67.8	59.2	60.6
SegLLM (ours)	**79.7**	**70.0**	**72.2**	**80.2**	**70.3**	**72.6**	**80.4**	**70.7**	**72.3**	**78.6**	**69.0**	**71.6**
vs. prev. SOTA	**+9.6**	**+9.0**	**+9.1**	**+12.4**	**+11.3**	**+10.2**	**+5.7**	**+5.8**	**+6.2**	**+3.7**	**+3.9**	**+3.7**

Table 7: SegLLM Exhibits greater robustness to a variety of question templates in image reasoning segmentation. Unlike previous models such as LISA (Lai et al., 2024) and SESAME (Wu et al., 2024), which tend to overfit to specific question templates encountered during training, SegLLM demonstrates improved robustness. We assess performance using the single-round RefCOCO dataset with cumulative cIoU as the evaluation metric. Notably, the templates used for evaluation were not utilized during the model training process.

Mask-enc	Box-enc	Ref Loss	**Single-Round** RefCOCO / + / g	**Multi-Round** RefCOCO / + / g	**Multi-Round (hard)** RefCOCO / + / g
✗	✗	✗	80.2 / 67.1 / 70.8	59.6 / 53.9 / 55.2	32.4 / 32.3 / 34.1
✓	✗	✗	83.6 / 73.0 / 77.7	72.2 / 68.1 / 68.1	58.6 / 58.6 / 59.1
✗	✓	✗	81.9 / 72.7 / 77.2	71.2 / 66.9 / 65.0	56.7 / 56.5 / 51.0
✓	✓	✗	82.3 / 72.2 / **77.8**	**75.7** / **71.3** / 68.6	67.6 / 67.3 / 62.8
✓	✓	✓	**83.8** / **72.5** / 76.7	74.0 / 70.1 / **65.8**	**69.6** / **69.4** / **63.7**

Table 8: Ablation study on the effectiveness of proposed components. Model performance evaluated on three benchmarks: (1) **Single-Round**—Referring segmentation in a single round using standard RefCOCO, RefCOCO+, and RefCOCOg datasets. (2) MRSeg: **Multi-Round**—Referring segmentation over multiple rounds, based on our custom benchmarks from RefCOCO, RefCOCO+, and RefCOCOg datasets (results show a weighted average of standard and hard subsets). (3) MRSeg (Hard): **Multi-Round (Hard)**—Focuses exclusively on the hard subset of the multi-round segmentation benchmarks. The evaluation metric used is CIoU.

performance across three subsets of the MR-RefCOCO dataset: 1) *Single-round*: single round referring segmentation using the standard RefCOCO/+/g datasets. 2) *MRSeg*: multi-round referring segmentation based on our MRSeg. 63) *MRSeg (Hard)*: this subset focuses exclusively on the hard subset of the MRSeg benchmarks, where understanding the reference mask is crucial for accurately segmenting the correct object. We provide more details for MRSeg (hard) in Appendix A.5. Our proposed components lead to a significant 20% performance improvement over the baseline. In the MRSeg (hard) subset, our mask-encoding scheme achieves over 30 points higher cIoU than the baseline, which highlight the effectiveness of our approach in enabling the model to interpret visual cues from user instructions and perform mask-conditioned segmentation—critical for handling complex tasks where reference masks, rather than text-based instructions, provide key information.

The proposed components also improve results on single-round referring segmentation as shown in Table 8. This achievement is noteworthy as the task does not explicitly require box-encoding and mask-encoding. We hypothesize that the absence of these encoding modules complicates the learning of segmentation from multi-round instructions, resulting in less stable training dynamics that affect performance even in single-round tasks.

Fine-tuning LISA's method on our multi-round datasets. Since the baseline setting in the first row in Table 8 is architecturally equivalent to LISA's method, this evaluation result is illustrative of the performance of LISA's method when trained on the same split of MR-RefCOCO and using same training method as our model. Hence, the ablation study shows that the mask and box encoders as well as the reference mask loss are indeed necessary components for achieving good performance on our multi-round segmentation task, and simply training previous methods without these components on our data alone is not sufficient to bridge this gap.

6 Conclusions

We introduce SegLLM, a novel multi-round interactive reasoning segmentation model that enhances traditional segmentation models by retaining conversational memory of visual, not just textual, results. Utilizing a mask-aware multimodal large language model, SegLLM integrates previous segmentation outputs back into its input stream, allowing it to handle complex queries about relationships between objects across multiple interactions. Tested on the newly curated MRSeg, SegLLM significantly outperforms existing benchmarks in multi-round interactive segmentation by over 20% and shows a 4.7% improvement in single-round referring segmentation. These results demonstrate SegLLM's capability as a versatile model for a broad range of instruction-following segmentation tasks.

References

Josh Achiam, Steven Adler, Sandhini Agarwal, Lama Ahmad, Ilge Akkaya, Florencia Leoni Aleman, Diogo Almeida, Janko Altenschmidt, Sam Altman, Shyamal Anadkat, et al. Gpt-4 technical report. *arXiv preprint arXiv:2303.08774*, 2023. 1

Jean-Baptiste Alayrac, Jeff Donahue, Pauline Luc, Antoine Miech, Iain Barr, Yana Hasson, Karel Lenc, Arthur Mensch, Katherine Millican, Malcolm Reynolds, et al. Flamingo: a visual language model for few-shot learning. *Advances in neural information processing systems*, 35:23716–23736, 2022. 1, 3

Anas Awadalla, Irena Gao, Josh Gardner, Jack Hessel, Yusuf Hanafy, Wanrong Zhu, Kalyani Marathe, Yonatan Bitton, Samir Gadre, Shiori Sagawa, et al. Openflamingo: An open-source framework for training large autoregressive vision-language models. *arXiv preprint arXiv:2308.01390*, 2023. 1, 3

Tom Brown, Benjamin Mann, Nick Ryder, Melanie Subbiah, Jared D Kaplan, Prafulla Dhariwal, Arvind Neelakantan, Pranav Shyam, Girish Sastry, Amanda Askell, et al. Language models are few-shot learners. *Advances in neural information processing systems*, 33:1877–1901, 2020. 2

Holger Caesar, Jasper R. R. Uijlings, and Vittorio Ferrari. Coco-stuff: Thing and stuff classes in context. *2018 IEEE/CVF Conference on Computer Vision and Pattern Recognition*, pp. 1209–1218, 2016. URL `https://api.semanticscholar.org/CorpusID:4396518`. 4

Keqin Chen, Zhao Zhang, Weili Zeng, Richong Zhang, Feng Zhu, and Rui Zhao. Shikra: Unleashing multimodal llm's referential dialogue magic. *arXiv preprint arXiv:2306.15195*, 2023. 3, 8

Bowen Cheng, Ishan Misra, Alexander G Schwing, Alexander Kirillov, and Rohit Girdhar. Masked-attention mask transformer for universal image segmentation. In *Proceedings of the IEEE/CVF conference on computer vision and pattern recognition*, pp. 1290–1299, 2022. 1

Aakanksha Chowdhery, Sharan Narang, Jacob Devlin, Maarten Bosma, Gaurav Mishra, Adam Roberts, Paul Barham, Hyung Won Chung, Charles Sutton, Sebastian Gehrmann, et al. Palm: Scaling language modeling with pathways. *Journal of Machine Learning Research*, 24(240):1–113, 2023. 2

Wenliang Dai, Junnan Li, Dongxu Li, Anthony Meng Huat Tiong, Junqi Zhao, Weisheng Wang, Boyang Li, Pascale N Fung, and Steven Hoi. Instructblip: Towards general-purpose vision-language models with instruction tuning. *Advances in Neural Information Processing Systems*, 36, 2024. 1, 3

Daan de Geus, Panagiotis Meletis, Chenyang Lu, Xiaoxiao Wen, and Gijs Dubbelman. Part-aware panoptic segmentation. In *Proceedings of the IEEE/CVF Conference on Computer Vision and Pattern Recognition*, pp. 5485–5494, 2021. 4

Jacob Devlin, Ming-Wei Chang, Kenton Lee, and Kristina Toutanova. Bert: Pre-training of deep bidirectional transformers for language understanding. *arXiv preprint arXiv:1810.04805*, 2018. 1

Henghui Ding, Chang Liu, Suchen Wang, and Xudong Jiang. Vision-language transformer and query generation for referring segmentation. In *Proceedings of the IEEE/CVF International Conference on Computer Vision*, pp. 16321–16330, 2021. 7

Zheng Ding, Jieke Wang, and Zhuowen Tu. Open-vocabulary universal image segmentation with maskclip. In *Proceedings of the 40th International Conference on Machine Learning*, pp. 8090–8102, 2023. 1

Agrim Gupta, Piotr Dollar, and Ross Girshick. Lvis: A dataset for large vocabulary instance segmentation. In *Proceedings of the IEEE/CVF conference on computer vision and pattern recognition*, pp. 5356–5364, 2019. 4, 6

Kaiming He, Georgia Gkioxari, Piotr Dollár, and Ross Girshick. Mask r-cnn. In *Proceedings of the IEEE international conference on computer vision*, pp. 2961–2969, 2017. 1

Jordan Hoffmann, Sebastian Borgeaud, Arthur Mensch, Elena Buchatskaya, Trevor Cai, Eliza Rutherford, Diego de Las Casas, Lisa Anne Hendricks, Johannes Welbl, Aidan Clark, et al. Training compute-optimal large language models. *arXiv preprint arXiv:2203.15556*, 2022. 2

Albert Q Jiang, Alexandre Sablayrolles, Arthur Mensch, Chris Bamford, Devendra Singh Chaplot, Diego de las Casas, Florian Bressand, Gianna Lengyel, Guillaume Lample, Lucile Saulnier, et al. Mistral 7b. *arXiv preprint arXiv:2310.06825*, 2023. 1

Sahar Kazemzadeh, Vicente Ordonez, Mark Matten, and Tamara Berg. Referitgame: Referring to objects in photographs of natural scenes. In *Proceedings of the 2014 conference on empirical methods in natural language processing (EMNLP)*, pp. 787–798, 2014. 4

Alexander Kirillov, Eric Mintun, Nikhila Ravi, Hanzi Mao, Chloe Rolland, Laura Gustafson, Tete Xiao, Spencer Whitehead, Alexander C Berg, Wan-Yen Lo, et al. Segment anything. *arXiv preprint arXiv:2304.02643*, 2023. 3, 4, 6

Ranjay Krishna, Yuke Zhu, Oliver Groth, Justin Johnson, Kenji Hata, Joshua Kravitz, Stephanie Chen, Yannis Kalantidis, Li-Jia Li, David A Shamma, et al. Visual genome: Connecting language and vision using crowdsourced dense image annotations. *International journal of computer vision*, 123:32–73, 2017. 4

Xin Lai, Zhuotao Tian, Yukang Chen, Yanwei Li, Yuhui Yuan, Shu Liu, and Jiaya Jia. Lisa: Reasoning segmentation via large language model. In *Proceedings of the IEEE/CVF Conference on Computer Vision and Pattern Recognition*, pp. 9579–9589, 2024. 1, 2, 3, 7, 8, 9, 10

Teven Le Scao, Angela Fan, Christopher Akiki, Ellie Pavlick, Suzana Ilić, Daniel Hesslow, Roman Castagné, Alexandra Sasha Luccioni, François Yvon, Matthias Gallé, et al. Bloom: A 176b-parameter open-access multilingual language model. 2023. 2

Bo Li, Yuanhan Zhang, Liangyu Chen, Jinghao Wang, Jingkang Yang, and Ziwei Liu. Otter: A multi-modal model with in-context instruction tuning, 2023a. 3

Junnan Li, Dongxu Li, Silvio Savarese, and Steven Hoi. Blip-2: Bootstrapping language-image pre-training with frozen image encoders and large language models. In *International conference on machine learning*, pp. 19730–19742. PMLR, 2023b. 3

Tsung-Yi Lin, Michael Maire, Serge Belongie, James Hays, Pietro Perona, Deva Ramanan, Piotr Dollár, and C Lawrence Zitnick. Microsoft coco: Common objects in context. In *Computer Vision–ECCV 2014: 13th European Conference, Zurich, Switzerland, September 6-12, 2014, Proceedings, Part V 13*, pp. 740–755. Springer, 2014a. 6

Tsung-Yi Lin, Michael Maire, Serge J. Belongie, James Hays, Pietro Perona, Deva Ramanan, Piotr Dollár, and C. Lawrence Zitnick. Microsoft coco: Common objects in context. In *European Conference on Computer Vision*, 2014b. URL https://api.semanticscholar.org/CorpusID:14113767. 4

Haotian Liu, Chunyuan Li, Qingyang Wu, and Yong Jae Lee. Visual instruction tuning. *Advances in neural information processing systems*, 36, 2024. 1, 3, 6

Ilya Loshchilov and Frank Hutter. Decoupled weight decay regularization. *arXiv preprint arXiv:1711.05101*, 2017. 1

Maxime Oquab, Timothée Darcet, Théo Moutakanni, Huy Vo, Marc Szafraniec, Vasil Khalidov, Pierre Fernandez, Daniel Haziza, Francisco Massa, Alaaeldin El-Nouby, et al. Dinov2: Learning robust visual features without supervision. *arXiv preprint arXiv:2304.07193*, 2023. 3

Zhiliang Peng, Wenhui Wang, Li Dong, Yaru Hao, Shaohan Huang, Shuming Ma, and Furu Wei. Kosmos-2: Grounding multimodal large language models to the world. *arXiv preprint arXiv:2306.14824*, 2023. 3

Renjie Pi, Jiahui Gao, Shizhe Diao, Rui Pan, Hanze Dong, Jipeng Zhang, Lewei Yao, Jianhua Han, Hang Xu, and Lingpeng Kong Tong Zhang. Detgpt: Detect what you need via reasoning. *arXiv preprint arXiv:2305.14167*, 2023a. 1, 3

Renjie Pi, Lewei Yao, Jiahui Gao, Jipeng Zhang, and Tong Zhang. Perceptiongpt: Effectively fusing visual perception into llm. *arXiv preprint arXiv:2311.06612*, 2023b. 3

Alec Radford, Jong Wook Kim, Chris Hallacy, Aditya Ramesh, Gabriel Goh, Sandhini Agarwal, Girish Sastry, Amanda Askell, Pamela Mishkin, Jack Clark, et al. Learning transferable visual models from natural language supervision. In *International conference on machine learning*, pp. 8748–8763. PMLR, 2021. 1, 3, 6

Vignesh Ramanathan, Anmol Kalia, Vladan Petrovic, Yi Wen, Baixue Zheng, Baishan Guo, Rui Wang, Aaron Marquez, Rama Kovvuri, Abhishek Kadian, et al. Paco: Parts and attributes of common objects. In *Proceedings of the IEEE/CVF Conference on Computer Vision and Pattern Recognition*, pp. 7141–7151, 2023. 4, 6

Hanoona Rasheed, Muhammad Maaz, Sahal Shaji, Abdelrahman Shaker, Salman Khan, Hisham Cholakkal, Rao M Anwer, Eric Xing, Ming-Hsuan Yang, and Fahad S Khan. Glamm: Pixel grounding large multimodal model. In *Proceedings of the IEEE/CVF Conference on Computer Vision and Pattern Recognition*, pp. 13009–13018, 2024. 7, 8

Jeff Rasley, Samyam Rajbhandari, Olatunji Ruwase, and Yuxiong He. Deepspeed: System optimizations enable training deep learning models with over 100 billion parameters. In *Proceedings of the 26th ACM SIGKDD International Conference on Knowledge Discovery & Data Mining*, pp. 3505–3506, 2020. 1

Gemini Team, Rohan Anil, Sebastian Borgeaud, Yonghui Wu, Jean-Baptiste Alayrac, Jiahui Yu, Radu Soricut, Johan Schalkwyk, Andrew M Dai, Anja Hauth, et al. Gemini: a family of highly capable multimodal models. *arXiv preprint arXiv:2312.11805*, 2023. 1

Hugo Touvron, Thibaut Lavril, Gautier Izacard, Xavier Martinet, Marie-Anne Lachaux, Timothée Lacroix, Baptiste Rozière, Naman Goyal, Eric Hambro, Faisal Azhar, et al. Llama: Open and efficient foundation language models. *arXiv preprint arXiv:2302.13971*, 2023. 1, 2, 3

Wenhai Wang, Zhe Chen, Xiaokang Chen, Jiannan Wu, Xizhou Zhu, Gang Zeng, Ping Luo, Tong Lu, Jie Zhou, Yu Qiao, et al. Visionllm: Large language model is also an open-ended decoder for vision-centric tasks. *Advances in Neural Information Processing Systems*, 36, 2024a. 8

Xudong Wang, Shufan Li, Konstantinos Kallidromitis, Yusuke Kato, Kazuki Kozuka, and Trevor Darrell. Hierarchical open-vocabulary universal image segmentation. *Advances in Neural Information Processing Systems*, 36, 2024b. 1, 6

Ronald J Williams and David Zipser. A learning algorithm for continually running fully recurrent neural networks. *Neural computation*, 1(2):270–280, 1989. 1

Tsung-Han Wu, Giscard Biamby, David Chan, Lisa Dunlap, Ritwik Gupta, Xudong Wang, Joseph E Gonzalez, and Trevor Darrell. See say and segment: Teaching lmms to overcome false premises. In *Proceedings of the IEEE/CVF Conference on Computer Vision and Pattern Recognition*, pp. 13459–13469, 2024. 1, 9, 10

Jianwei Yang, Hao Zhang, Feng Li, Xueyan Zou, Chunyuan Li, and Jianfeng Gao. Set-of-mark prompting unleashes extraordinary visual grounding in gpt-4v. *arXiv preprint arXiv:2310.11441*, 2023a. 3

Zhao Yang, Jiaqi Wang, Yansong Tang, Kai Chen, Hengshuang Zhao, and Philip HS Torr. Lavt: Language-aware vision transformer for referring image segmentation. In *Proceedings of the IEEE/CVF Conference on Computer Vision and Pattern Recognition*, pp. 18155–18165, 2022. 7

Zhengyuan Yang, Linjie Li, Kevin Lin, Jianfeng Wang, Chung-Ching Lin, Zicheng Liu, and Lijuan Wang. The dawn of lmms: Preliminary explorations with gpt-4v (ision). *arXiv preprint arXiv:2309.17421*, 9(1):1, 2023b. 3

Qinghao Ye, Haiyang Xu, Guohai Xu, Jiabo Ye, Ming Yan, Yiyang Zhou, Junyang Wang, Anwen Hu, Pengcheng Shi, Yaya Shi, et al. mplug-owl: Modularization empowers large language models with multimodality. *arXiv preprint arXiv:2304.14178*, 2023. 3

Shukang Yin, Chaoyou Fu, Sirui Zhao, Ke Li, Xing Sun, Tong Xu, and Enhong Chen. A survey on multimodal large language models. *arXiv preprint arXiv:2306.13549*, 2023. 3

Haoxuan You, Haotian Zhang, Zhe Gan, Xianzhi Du, Bowen Zhang, Zirui Wang, Liangliang Cao, Shih-Fu Chang, and Yinfei Yang. Ferret: Refer and ground anything anywhere at any granularity. *arXiv preprint arXiv:2310.07704*, 2023. 3

Licheng Yu, Patrick Poirson, Shan Yang, Alexander C Berg, and Tamara L Berg. Modeling context in referring expressions. In *Computer Vision–ECCV 2016: 14th European Conference, Amsterdam, The Netherlands, October 11-14, 2016, Proceedings, Part II 14*, pp. 69–85. Springer, 2016. 4, 6

Andy Zeng, Maria Attarian, Brian Ichter, Krzysztof Choromanski, Adrian Wong, Stefan Welker, Federico Tombari, Aveek Purohit, Michael Ryoo, Vikas Sindhwani, et al. Socratic models: Composing zero-shot multimodal reasoning with language. *arXiv preprint arXiv:2204.00598*, 2022. 3

Ao Zhang, Liming Zhao, Chen-Wei Xie, Yun Zheng, Wei Ji, and Tat-Seng Chua. Next-chat: An lmm for chat, detection and segmentation. *arXiv preprint arXiv:2311.04498*, 2023a. 1, 3

Ao Zhang, Yuan Yao, Wei Ji, Zhiyuan Liu, and Tat-Seng Chua. NExt-chat: An LMM for chat, detection and segmentation. In *Forty-first International Conference on Machine Learning*, 2024. 7, 8

Shilong Zhang, Peize Sun, Shoufa Chen, Min Xiao, Wenqi Shao, Wenwei Zhang, Kai Chen, and Ping Luo. Gpt4roi: Instruction tuning large language model on region-of-interest. *arXiv preprint arXiv:2307.03601*, 2023b. 3

Bolei Zhou, Hang Zhao, Xavier Puig, Sanja Fidler, Adela Barriuso, and Antonio Torralba. Scene parsing through ade20k dataset. *2017 IEEE Conference on Computer Vision and Pattern Recognition (CVPR)*, pp. 5122–5130, 2017. URL https://api.semanticscholar.org/CorpusID:5636055. 4

Deyao Zhu, Jun Chen, Xiaoqian Shen, Xiang Li, and Mohamed Elhoseiny. Minigpt-4: Enhancing vision-language understanding with advanced large language models. *arXiv preprint arXiv:2304.10592*, 2023. 3

Xueyan Zou, Jianwei Yang, Hao Zhang, Feng Li, Linjie Li, Jianfeng Gao, and Yong Jae Lee. Segment everything everywhere all at once. *arXiv preprint arXiv:2304.06718*, 2023. 7

A APPENDIX

A.1 TRAINING DETAILS

We use NVIDIA A100 GPUs for model training. We fine-tune our model with a total batch size of 16 (a per-device batch size of 2) using the AdamW optimizer (Loshchilov & Hutter, 2017) with a learning rate of $2e^{-5}$. Furthermore, we utilize stage-2 DeepSpeed accelerator (Rasley et al., 2020) and bf16 floating point precision to enhance training efficiency and reduce memory consumption.

A.2 QUESTION TEMPLATES GENERATION

We observed that current state-of-the-art chat-based image segmentation models, such as LISA (Lai et al., 2024), tend to rely heavily on a fixed set of question templates. This leads to fluctuations and instability in segmentation quality when user prompts are phrased differently, suggesting potential overfitting to specific language prompts.

To address this, we leveraged the web-version of GPT-4 (Achiam et al., 2023) to generate diverse templates, creating more natural language conversations from dataset annotations. We generated templates for direct referring segmentation queries, relational queries, and hierarchical queries. For each query type, we created 100$\sim$200 templates for training and 50$\sim$100 different templates for validation.

A.3 MASK AND BOX ENCODING DETAILS

To obtain the mask embedding, we first set the pixels outside the reference mask as black, then we crop the image according to the bounding box of the reference mask. This yields an object-centric image of the masked object. We then pass this image to a CLIP-ViT encoder (Radford et al., 2021), and obtain the raw mask embedding. We use an MLP layer to map this embedding to the input dimension of LLMs.

To obtain the bounding box embedding, we first compute the bounding box coordinates using the generated mask, then we create a positional embedding whose dimension matches the input dimension of LLM. We use this generated positional embedding as the final bounding box embedding.

For each mask, we obtain the two embeddings and feed them sequentially back to the input stream of LLMs. Following LISA, we use a [SEG] token to generate the masks. During the training process, we employ the teacher enforcing (Williams & Zipser, 1989) and directly append the ground truth mask and bounding box embedding after each [SEG] token. At the inference time, we compute the two embeddings for each mask generate and insert the embeddings before the input for the next round.

A.4 LISA EVALUATION PROTOCOL DISCUSSION

When exploring different protocols to evaluated LISA on our multi-round dataset, we find that LISA performs worse using approach 2 and 3, when compared to approach 1, despite the inclusion of the additional information such as the caption of the reference instance or the painted reference mask compared to the word "mask". We suspect that this may be due to LISA being trained on data that focuses on 1 instance, hence the presence of description for two instances, the target and the reference instance, may cause more confusion than guidance. In addition, the painting the reference instance to a different color may cause a distribution shift in the input image.

In the 3rd approach, we averaged the result across painting the mask in three different colors, red, green and yellow. We found that changing the color did not make a significant difference, as the standard deviation across three colors is ≤ 1 point. We use cumulative intersection-over-union (cIoU) metric as the evaluation metric, which is the cumulative intersection over the cumulative union: $\frac{\sum_{i=1}^{N} \text{Intersection}_i}{\sum_{i=1}^{N} \text{Union}_i}$, where Intersection_i is the number of pixels in the intersecting region of the predicted mask and the ground truth mask for image i, and Union_i is the number of pixels in the union of the predicted mask and the ground truth mask for image i. By contrast, mIoU is defined by $\frac{1}{N}\sum_{i=1}^{N}\frac{\text{Intersection}_i}{\text{Union}_i}$

A.5 Dataset Details

In the section, we document further details on the dataset construction process. We also provide some statistics about our dataset.

A.5.1 Dataset Size

We document the number of images sampled from each source dataset and the number of conversations generated in Table A1. Additionally, we visualize the distribution of the number of rounds for each dataset in Fig. A1.

Datasets	Training Set			Validation Set		
	# of Convs	# of Images	Max Rounds	# of Convs	# of Images	Max Rounds
RefCOCO(+/g)	55188	27674	18	4263	2701	17
Visual Genome	367674	94221	2	40980	10524	2
PACO-LVIS	40827	40827	19	2178	2178	16
LVIS	71388	71255	17	13898	13898	18
Pascal Panoptic Part	4577	4577	17	4690	4690	18
ADE20K	59784	20196	1	5943	200	1
COCO-Stuff	340127	118205	1	14461	4999	1
Attributes-COCO	49036	36413	1	5000	2566	1
ReasonSeg	1326	239	1	200	200	1
MRSeg (hard)	22470	22470	1	1988	1988	1

Table A1: Statistics of our MRSeg dataset, including the number of overall conversations, number of images, and the maximum rounds of conversations for each dataset after processing through our dataset pipeline.

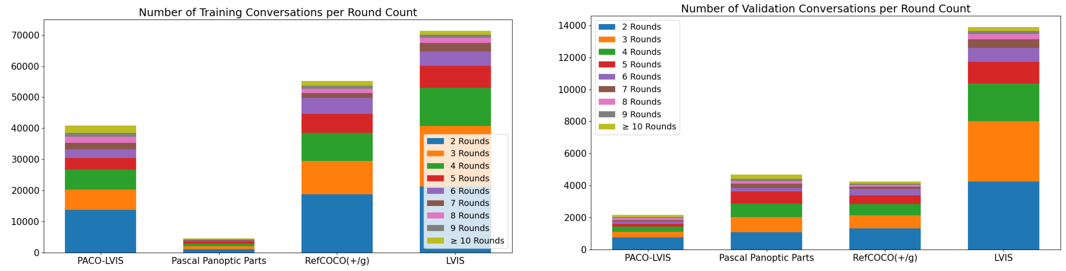

Figure A1: Bar-plot visualization for training and validation conversations count at different number of rounds for multi-round datasets. There are very conversations with a large number of rounds.

A.5.2 Conversation Generation Pipeline

We employ different strategies to generate natural-language conversation for different source datasets. Specifically, our dataset is generated using a combination of the following methods:

- ***Hierarchical relationships based on PACO-LVIS and Pascal Panoptic Part***: In these queries, the model is asked to segment objects which are a sub-part of some output of a previous round. From each image, we randomly sample between one and four instances, and for each instance, we randomly sample between one and four parts. We initiate queries about the instance followed by questions targeting the parts of each respective instance. For Pascal Panoptic Part, we only use objects and their parts on a instance level and not a semantic segmentation level to avoid ambiguity. For both PACO-LVIS and Pascal Panoptic Part, we refer to previous round outputs with it's actual caption, e.g. ``the knife'' with probablility 50%. With the other 50% we refer to the previous round output as ``<instance i>'' or ``<the output of round i>''.
- ***Positional relationships based on Refcoco(+/g) and LVIS***: These conversations task the system with segmenting objects based on their positional relationships to the outputs from previous rounds.We randomly sample between 2 to 18 annotations per image. For each selected annotation, we either generate a query about the object itself or generate a query involving an object from previously processed instances, focusing on their relative positions calculated from their bounding box coordinates. For RefCOCO(+/g), multiple annotations may be selected for the same instance

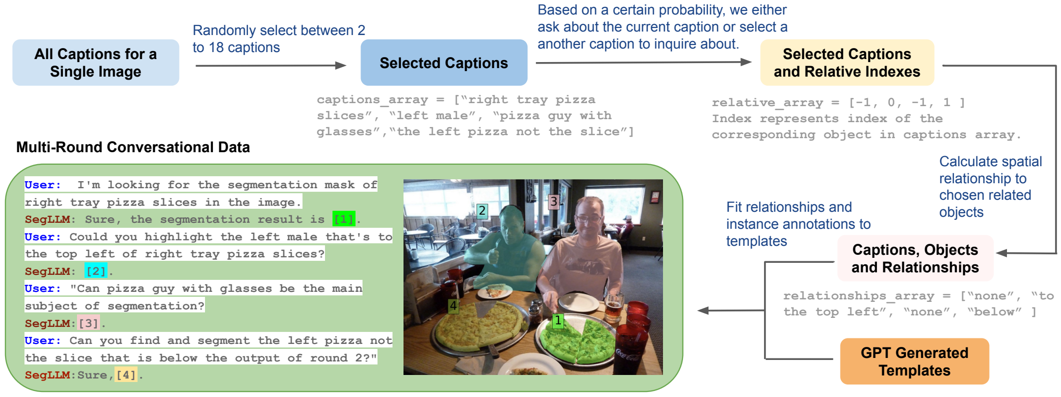
All Captions for a Single Image
Randomly select between 2 to 18 captions
Selected Captions
captions_array = ["right tray pizza slices", "left male", "pizza guy with glasses","the left pizza not the slice"]
Based on a certain probability, we either ask about the current caption or select a another caption to inquire about.
Selected Captions and Relative Indexes
relative_array = [-1, 0, -1, 1] Index represents index of the corresponding object in captions array.
Calculate spatial relationship to chosen related objects
Captions, Objects and Relationships
Fit relationships and instance annotations to templates
relationships_array = ["none", "to the top left", "none", "below"]
GPT Generated Templates
Multi-Round Conversational Data
2
3
4
1

```
User:  I'm looking for the segmentation mask of right tray pizza slices in the image.
SegLLM: Sure, the segmentation result is [1].
User: Could you highlight the left male that's to the top left of right tray pizza slices?
SegLLM: [2].
User: "Can pizza guy with glasses be the main subject of segmentation?
SegLLM:[3].
User: Can you find and segment the left pizza not the slice that is below the output of round 2?"
SegLLM:Sure,[4].
```

Figure A2: Pipeline for generating multi-round conversational data for RefCOCO(+/g) in MRSeg.

due to multiple captions available per instance.For LVIS, we select annotations where only one or two objects of that class appear in the image. When two objects of the same class are present, we detail their relative positions and add location descriptions to their captions to prevent ambiguity. We specifically choose instances not categorized under COCO classes to diversify the dataset's class variety. The probability for each round to query about an object itself is $1/3$, otherwise, we query about the current object with a reference to a previous round's output and their relative position. To assign the positional relationships, we use compare the edge and center position of the bounding boxes for the two instance we are trying to assign a relationship to. There are 9 total possible positions two instances can have (the same as, overlapping with, to the left/right, above/below, to the top/bottom left/right of). Similar to Hierarchical Queries,we refer to previous round outputs with it's actual caption, e.g. ``the woman on the left'' with probablility 50%. With the other 50% we refer to the previous round output as ``<instance i>'' or ``<the output of round i>''. A detailed pipeline for how RefCOCO(+/g) dataset is sampled can be see in Fig. A2

- ***MR Seg(hard)***: For each RefCOCO image, we identify cases where there are two instances of the same class within the image. From these, we select a pair of instances and construct two single-round conversations. Given two instances, X and Y, of the same class in the image, we create the following conversations:

  – Conv 1: `[IMAGE] [ENCODE X] Please segment the other <class name>` → `Sure, [DECODE Y]`

  – Conv 2: `[IMAGE] [ENCODE Y] Please segment the other <class name>` → `Sure, [DECODE X]`

  We have 10 different templates for the training and 5 templates validation/test for MR Seg(hard).

- ***Interactional relationships based on Visual Genome***: We adopt Visual Genome (VG), utilizing its relationship annotations to construct conversations that emphasize interactional dynamics rather than merely positional relationships. We sample up to four relationships per image. Each relationship prompts a two-round conversation: the first round involves segmenting the subject, and the second round involves segmenting an object based on its relationship to the subject. Since VG also only provides bounding box labels, we generate masks for selected instances using SAM.

A.5.3 Details of GPT4 Usage

We prompt GPT-4 models for generating captions for attribute-based descriptions as well as for cleaning grammar errors in our dataset. The detailed instructions and specific model we used can be found in Table A2 and Table A3. For the attribute-based description, we crop COCO images to only contain the specified instance, feeding the cropped image and it's class name to GPT to generate a description. For language correction, we found that grammar correction is often erroneous but can be a lot of accurate if we go through the data twice to double check.

```
payload = {
    "model": "gpt-4-turbo-2024-04-09",
    "messages": [
      {
        "role": "user",
        "content": [
          {
            "type": "text",
            "text": f"Can you focus on describing the {class_name} in
                the image? Can you format your output in a two item
                array, such that the first index is an abstract
                description without any class name, such as ’has a pizza
                sitting on top of it’ or ’is wearing a beige t-shirt’
                and the second index is the exact classname for the
                object, such as ’a dining table’ or ’a man’."
          },
          {
            "type": "image_url",
            "image_url": {
              "url": f"data:image/jpeg;base64,{base64_image}",
              "detail": "low"
            }
          }
        ]
      }
    ],
    "max_tokens": 200
  }
```

Table A2: Our full prompt to the GPT-4-turbo-2024-04-09 model for generating abstract descriptions

A.5.4 More discussions on demo outputs

In Fig. A3, example **A** illustrate the necessity of our Mask-Encoding Scheme, to avoid the ambiguity that may arise in cases where multiple instances of the same class are present in the image. Round 2 and round 3 in example **A** show that without our mask encoding mechanism to supply information about the person segmented from round 1, since there are multiple laptops and chairs present in the image, confusion arises as to which specific laptop or chair the user is referring to in the query prompt. Therefore, without the guiding information from the mask encoding, LISA seems to naively guess the incorrect laptop in round 2, and does not generate a comprehensible segmentation mask in round 3. In contrast, the mask encoding guides our model to correctly segment the requested objects. Similarly, in round 4 and round 6, our model was able to successfully segment the keyboard of the laptop from round 3 and the person setting on the chair from round 5.

This phenomenon is again demonstrated in **B** in Fig. A3. Since there are two women, both carrying bags and holding an umbrella in the image, our Mask-Encoding Scheme again resolves this the ambiguity and allows the user to conveniently specify the bag and the umbrella requested in round 2 and round 3 are carried and held by the person from round 1. As before, the awareness of previous round outputs enables our model to segment the correct objects, whereas LISA guesses the incorrect objects due to the lack of this awareness.

Example **C** demonstrates that our model is not limited to multi-round prompting, and can produce accurate segmentation results via direct, single-round prompts as well. In the indirect case, we first ask the model to segment the dog during the first round of the conversation. Then, in the second round, we ask a follow up question to guide the model to segment the Frisbee that is caught by the dog from round 1. However, tin the direct case, we straight away ask for the Frisbee that is caught by the dog. In comparison, our model succeeds in both the direct and indirect case, whereas LISA fails to segment the correct Frisbee instance in either cases. This shows that our multi-round comprehension capability is not a limitation but an addition.

```
Round 1:
response = client.chat.completions.create(
            model="gpt-4o-2024-05-13",
            response_format={ "type": "json_object" },
            messages=[
                {"role": "system", "content": "You are a helpful
                    assistant designed to output JSON."},
                {"role": "user", "content": f"Can you fix any errors and
                    make the sentence sound like natural English, and
                    provide our output in a dictionary of format
                    ’corrected’=CORRECT_SENTENCE? here is the sentence I
                    want you to correct, ’{sent}’"}
            ]
        )
Round 2:
    response = client.chat.completions.create(
            model="gpt-4o-2024-05-13",
            response_format={ "type": "json_object" },
            messages=[
                {"role": "system", "content": "You are a helpful
                    assistant designed to output JSON"},
                {"role": "user", "content": f"Here is the original
                    sentence: ’{sent}’. Here is the corrected sentence:
                    ’{corrected_sent}’. Does the corrected sentence have
                    the same meaning as the original? If yes, please
                    output [’Same’, ’None’]. If no, please output
                    [’Different’,
                    ’<corrected_with_same_meaning_as_original>’]."}
            ]
        )
```

Table A3: Out full prompt to the gpt-4o-2024-05-13 model for grammar correction. We use a two-round approach, feeding GPT’s first round answer back to itself to be self-corrected.

Lastly, we note that round 3 and round 6 of example **A**, round 2 and round 3 of example **B** and round 2 of example **C** demonstrate our model’s understanding of *interactional relationships* as introduced in Sec. 4.1 and round 4 demonstrates the *hierarchical relationship* introduced in Sec. 4.1.

B License

We makes use the following models: CLIP (MIT license), LLAMA 2 (Llama 2 Community License Agreement), Vicuna (Apache2 license). BLIP-2 (BSD-3-Clause license)

We use the following dataset COCO (Attribution-NonCommercial-ShareAlike 4.0 Internationa), RefCOCO (Apache-2.0 license), Visual Genome (Creative Commons Attribution 4.0 International License.), PACO (MIT License), Pascal-Panoptic-Parts (Apache-2.0 license), LIVIS (CC BY 4.0 + COCO license).

C Limitation

One limitation is that our model can only output a single mask, hence we are only able to perform segmentation on an instance level rather than a semantic level. Another limitation is that when the text input is ambiguous, our model may randomly select a possible output instead of asking which specific output is desires or output all possible options. This may be caused by the training data which is slightly noisy due to being converted from datasets not necessary for referring segmentation.

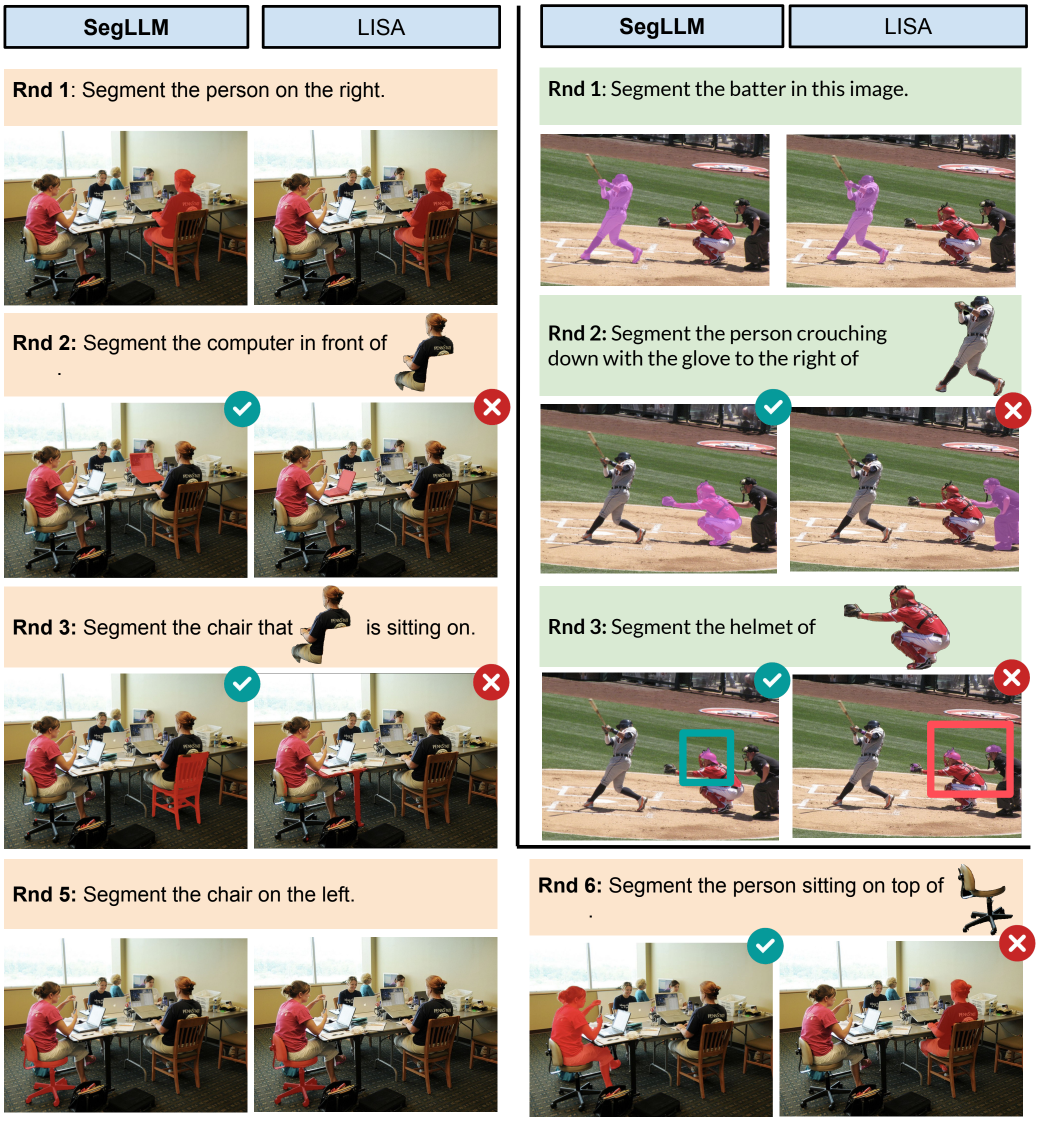
SegLLM
LISA
Rnd 1: Segment the person on the right.
Rnd 2: Segment the computer in front of .
Rnd 3: Segment the chair that is sitting on.
Rnd 5: Segment the chair on the left.
SegLLM
LISA
Rnd 1: Segment the batter in this image.
Rnd 2: Segment the person crouching down with the glove to the right of
Rnd 3: Segment the helmet of
Rnd 6: Segment the person sitting on top of .

Figure A3: Additional side-by-side comparison with LISA. This shows that without awareness of segmentation outputs from previous rounds, LISA struggles to identify the correct instance requested by the user, when there is ambiguity.

D Broader Impacts

Our paper imposes positive broader impacts. It can act as a educational tools. One can employ our model to demonstrate the relationship between objects by clearly segmenting them, this can help second-language speakers or children learn the meaning of different relationships, for example. It can also be beneficial for scientific research or environment monitoring. Our model can help detect extremely small objects autonomously simply with an image and text prompt.